Finite-difference complex-wavevector band structure solver for analysis and design of periodic radiative microphotonic structures

Jelena Notaros and Miloš A. Popović*

Department of Electrical, Computer, and Energy Engineering, University of Colorado, Boulder, Colorado 80309, USA
**Corresponding author: milos.popovic@colorado.edu*

Received January 26, 2015; accepted February 2, 2015;
posted February 6, 2015 (Doc. ID 232985); published March 11, 2015

We demonstrate a finite-difference approach to complex-wavevector band structure simulation and its use as a tool for the analysis and design of periodic leaky-wave photonic devices. With the (usually real) operating frequency and unit-cell refractive index distribution as inputs, the eigenvalue problem yields the complex-wavevector eigenvalues and Bloch modes of the simulated structure. In a two-dimensional implementation for transverse-electric fields with radiation accounted for by perfectly matched layer boundaries, we validate the method and demonstrate its use in simulating the complex-wavevector band structures and modal properties of a silicon photonic crystal waveguide, an array-antenna-inspired grating coupler with unidirectional radiation, and a recently demonstrated low-loss Bloch-mode-based waveguide crossing array. Additionally, we show the first direct solution of the recently proposed open-system low-loss Bloch modes. We expect this method to be a valuable tool in photonics design, enabling the rigorous analysis and synthesis of advanced periodic and quasi-periodic photonic devices.

OCIS codes: (050.1755) Computational electromagnetic methods; (130.3120) Integrated optics devices; (130.5296) Photonic crystal waveguides; (050.6624) Subwavelength structures.
http://dx.doi.org/10.1364/OL.40.001053

Periodic structures, such as photonic crystal microcavities and waveguides [1], fiber-to-chip grating couplers [2,3], and waveguide crossing arrays [4,5], are playing an increasingly important role in the design of integrated photonic circuits. With the prospect that silicon photonics can enable significant advances in a number of applications, including energy efficient processor-to-memory interconnects [6] and optical phased arrays [7], there is a need for efficient techniques for the rigorous design of periodic micro- and nanophotonic structures.

A natural way to design periodic photonic structures is through band structure analysis, i.e., Bloch–Floquet theory, using numerical solvers [8]. This approach allows rapid efficient design of most of the properties of a periodic structure through the design of a single unit cell. Since photonic band solvers typically take as input a real wavevector, k, absorbing or radiating structures are typically described by a computed complex-frequency and are effectively seen as a finite-quality-factor resonator. Furthermore, these solvers are unable to readily provide band structure information within bandgaps where the most natural picture involves a complex-wavevector; yet these bandgap fields are critical to the design of structures such as photonic crystal microcavities [1].

For devices designed to operate at a particular real driving frequency, complex-wavevector band structure analysis, with driving frequency provided at input, is the natural basis for physical intuition and rigorous analysis [9]. This is particularly true for propagation within the bandgaps of lossless structures (which do not appear in real-wavevector complex-frequency analysis) and for absorbing and leaky-wave radiative structures. For example, the optimization of grating couplers based on antenna-array concepts [3] implies a fixed real design frequency and optimization for radiation angle and decay rate—both computed from the complex-wavevector.

Furthermore, in our view, the complex-wavevector band structure picture could be particularly important for the design and synthesis of advanced "tapered-band-structure" devices, where unit cells with varying parameters are concatenated, all designed at a fixed real frequency of interest, to form a final device design. Such quasi-periodic structures with adiabatic tapering of the unit cell [10] have been employed to engineer high-quality-factor photonic crystal microcavities [1] and high-efficiency grating couplers [2]. Yet, their design has typically involved less than ideally suited tools such as finite-difference time-domain (FDTD) simulation or indirect complex-frequency band structure methods with analytical approximations in bandgaps [1]. Rigorous synthesis techniques are lacking, and band structure analysis appears to be inadequately adapted to date to these kinds of photonics design problems.

Recent work has investigated complex-wavevector band structure calculation in the context of modeling plasmonic/polaritonic structures to account for material absorption [11–14], as well as radiation loss through the incorporation of absorbing domain terminations such as perfectly matched layers [15].

In this Letter, we demonstrate a novel finite-difference complex-wavevector band structure solver with perfectly-matched-layer (PML) absorbing boundaries. We use the solver to compute the modal properties of two-dimensional radiating periodic photonic structures and suggest a vision for rigorous device synthesis based on such solvers. By utilizing a finite-difference method on a split Yee grid, our solver is robust since it is derived from self-consistent discrete electromagnetism with discrete conservation laws [16], enabling a complete orthogonal basis with no spurious solutions in the formulation. Furthermore, the solver's uniform grid allows for accurate simulation of coupled resonator physics

due to its consistent discretization of identical elements in the computational domain. This approach also makes the band structure solver directly integrable with FDTD and finite-difference waveguide mode solvers.

We first present the complex-wavevector electromagnetic eigenvalue problem formulation and implementation of the solver with PML boundary conditions and follow with validation of the method against an analytical solution. Next, we analyze the modal properties and band structures of a silicon linear photonic crystal waveguide, a unidirectional antenna-array-inspired fiber-to-chip grating coupler [3], and a low-loss Bloch-mode waveguide crossing array, where we demonstrate the first direct solution of the recently proposed open-system low-loss Bloch modes [4,5]. These examples illustrate the potential utility of a complex-wavevector band structure solver in device design.

Starting from Maxwell's equations, we derive the wave equation for the transverse electric field, $\Psi(x,y)$, of a two-dimensional structure,

$$[\partial_x^2+\partial_y^2+k_0^2n^2(x,y)]\Psi(x,y)=0, \tag{1}$$

where $k_0\equiv 2\pi f/c\equiv 2\pi/\lambda_0$ is the free-space wavenumber (related to wavelength, λ_0, and frequency, f) and $n(x,y)$ is the refractive index distribution of the structure. Notably, in our implementation, the refractive index may be real or complex, enabling simulation of dielectric, plasmonic, and other structures. For an index distribution that is periodic along x with periodicity a such that $n(x,y)=n(x+a,y)$, Bloch's theorem states that the field within the periodic medium can be represented as the product of an amplitude function periodic in x with the same periodicity as n, $\Phi(x,y)=\Phi(x+a,y)$, and a plane wave that carries the crystal momentum, k,

$$\Psi(x,y)=e^{ikx}\Phi(x,y). \tag{2}$$

Inserting Eq. (2) into Eq. (1), we obtain the wave equation for the periodic Bloch amplitude, $\Phi(x,y)$,

$$[\partial_x^2+\partial_y^2+i2k\partial_x-k^2+k_0^2n^2(x,y)]\Phi(x,y)=0, \tag{3}$$

which can be solved on a single unit cell of the structure. We then discretize this equation on the Yee interleaved grid [16,17] using the form

$$\left[\hat{\partial}_x\tilde{\partial}_x+\hat{\partial}_y\tilde{\partial}_y+i2k\frac{(\hat{\partial}_x+\tilde{\partial}_x)}{2}-k^2+k_0^2n_{m,n}^2\right]\Phi_{m,n}=0, \tag{4}$$

which is a quadratic eigenvalue problem with eigenvalue k and linear dependence on frequency (proportional to k_0). To allow solutions using standard sparse matrix techniques, we factor Eq. (4) into a linear eigenvalue problem of twice the size, using the linearization [14]

$$\begin{bmatrix}\boldsymbol{A} & \boldsymbol{B}\\ 0 & \boldsymbol{I}\end{bmatrix}\begin{bmatrix}\Phi\\ k\Phi\end{bmatrix}=k\begin{bmatrix}0 & -\boldsymbol{C}\\ \boldsymbol{I} & 0\end{bmatrix}\begin{bmatrix}\Phi\\ k\Phi\end{bmatrix}, \tag{5}$$

where $\boldsymbol{I}$ is the identity matrix and $\boldsymbol{A}$, $\boldsymbol{B}$, and $\boldsymbol{C}$ are matrix representations of the following operators derived from Eq. (4):

$$\hat{A}=\hat{\partial}_x\tilde{\partial}_x+\hat{\partial}_y\tilde{\partial}_y+k_0^2n_{m,n}^2,\ \hat{B}=i(\hat{\partial}_x+\tilde{\partial}_x),\ \hat{C}=-1. \tag{6}$$

The operator to sparse matrix translation is done using finite differences on a Yee grid [18]. The derived matrix operator yields a complete set of modes of the discrete system. Its sparsity allows efficient solution of the eigenproblem near a few modes of interest using standard sparse matrix techniques, the scaling of which is well known [18]. Note that the complex-wavevector problem matrix is doubled in size in comparison to the complex-frequency problem, owing to the need to linearize.

To enable the simulation of radiating structures, we introduce PML domain termination regions in transverse coordinate y utilizing complex-coordinate stretching [19]

$$\tilde{y}(y)=y+if(y), \tag{7}$$

$$f(y)=(y-y_T)^2u(y-y_T)+(y_B-y)^2u(y_B-y), \tag{8}$$

where the modified complex $\tilde{y}$ coordinate is a combination of real coordinate y and an imaginary function, with $f(y)\neq 0$ in the PML region. This modification ensures a reflectionless interface by analytic continuation of Maxwell's equations into the complex domain and transforms outgoing radiation into exponentially decaying waves in the PML region, thus allowing termination of the computational domain. Although these boundaries introduce unphysical "PML modes," these modes are essential to the PML's function, can be easily distinguished by their concentration of energy in the PML region, and add no practical limitations to our method.

To validate the presented theory and implementation, we compare numerical results obtained using the proposed solver to analytical solutions derived in literature [20]. We solve for the band structure of a two-material quarter-wave-stack medium using both one- and two-dimensional versions of the solver. A schematic of the medium and comparison of the resulting numerical and analytical band structures are shown in Fig. 1. With the complex-wavevector solver, varying the input frequency

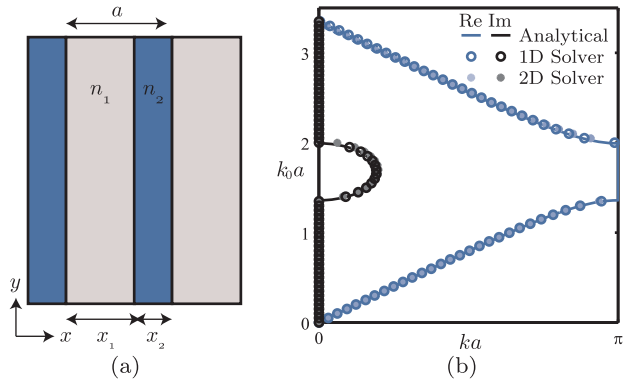

Fig. 1. (a) Periodic layered medium consisting of alternating layers of two materials with refractive indices n_1 and n_2 and thicknesses x_1 and x_2, respectively, and (b) comparison of numerical results obtained by the one- and two-dimensional versions of the proposed FDFD complex-wavevector solver with the analytical solution [20] for the medium's complex-k band structure. Re(k) is shown in blue and Im(k) in black. The periodic medium is a quarter-wave stack with $n_1=1.45$, $n_2=2.65$, $\lambda_0=1.5$ μm, $x_1=\lambda_0/(4n_1)$, and $x_2=\lambda_0/(4n_2)$.

(proportional to the normalized free-space wavenumber, k_0a) results in a variation of the normalized wavevector, ka, in both the real and the complex domains. In the first branch, when Re(k) reaches a value of π/a, the wavevector protrudes into the complex domain and bandgaps, representing the groups of frequencies not supported for propagation in the structure, are formed. Additionally, we observe from Fig. 1(b) an excellent agreement of numerical results obtained by both one- and two-dimensional solvers with the analytical solution. Analytically, the structure's bandgap size is computed to be $(\Delta k_0 a)_{\text{analytical}} \approx 0.634$ [20], whereas both one- and two-dimensional solvers yield $(\Delta k_0 a)_{\text{numerical}} \approx 0.635$ with slight differences in values attributed to discretization.

Next, we use the two-dimensional solver to demonstrate several applications of complex-wavevector band-structure analysis. We first simulate the band structure and multiple transverse electric field profiles of a periodic silicon photonic crystal waveguide as shown in Fig. 2. Figure 2(b) shows a unit cell of the structure which is periodic in coordinate x with periodicity a. The band structure, shown in Fig. 2(c), is computed

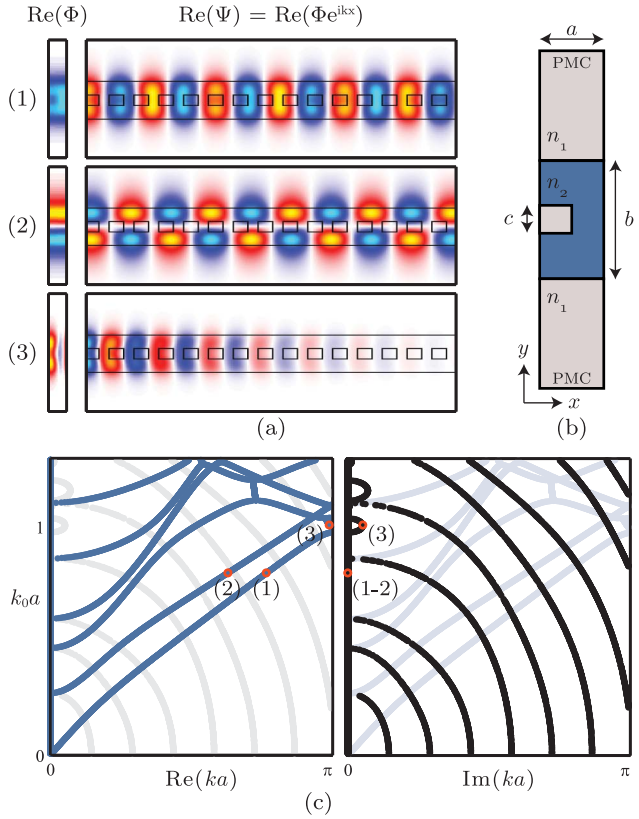

Fig. 2. (a) Mode profiles of the Bloch amplitude unit cell field Φ (left) and the full periodic structure field Ψ (right) for (1) the first-order dielectric, (2) the second-order dielectric, and (3) the bandgap modes of a periodic photonic crystal calculated using the proposed two-dimensional numerical solver. (b) Unit cell of the photonic crystal showing index distribution and dimensions. (c) Simulated complex-k band structure of the photonic crystal with Re(k) and Im(k) highlighted separately. The analyzed silicon photonic crystal is situated in silica and has square silica holes ($n_1 = 1.45$, $n_2 = 3.5$, $a = 330$ nm, $b = 700$ nm, and $c = 200$ nm). Points analyzed in (a) are marked on the band structure (c) in red.

by providing as input to the solver the normalized frequency, k_0a, and obtaining at output the complex-wavevector, ka, values and corresponding fields. Notably, modes are computed even in bandgaps, which traditional band solvers, with wavevector input, exclude. Fig. 2(a) shows the crystal's mode profile at three points on the band structure depicting both the Bloch amplitude unit cell field, Φ, and the full periodic structure field, $\Psi = e^{ikx}\Phi$. Points (1) and (2) in the figure are the first- and second-order modes, respectively, of the structure and exhibit conventional sinusoidal behavior. In contrast, at point (3), located in the photonic crystal's bandgap (i.e., in reflecting operation), the field, Ψ, undergoes the expected exponential decay along the propagation direction due to the imaginary component of k. This type of complex-wavevector simulation permits the rigorous computation of mirror strength design curves for the synthesis of high-quality-factor photonic crystal microcavities. Previously, such design was carried out using analytical circular dispersion curve approximations within the bandgap [1].

Complex-wavevector band-structure analysis is also ideally suited to the simulation and optimization of periodic fiber-to-chip grating couplers. Here, we simulate the leaky-wave Bloch modes and complex-wavevector band structure of a recently proposed unidirectionally-radiating grating coupler design inspired by antenna array concepts [3]. Figure 3(a) portrays the index distribution of three unit cells of the structure, and Fig. 3(b) shows the simulated Bloch modes of the grating demonstrating its radiation properties. To achieve unidirectional radiation, a two-element unit cell design is employed with each silicon tooth acting as a scatterer. The effective scattering centers of the teeth are separated in both x and y by about a quarter wavelength. This separation leads to constructive interference of the radiated field in one direction and destructive interference in the other, allowing for engineered unidirectional radiation [3]. Figure 3(b) shows that excitation from the left produces radiation up and back from the normal only, while excitation from the right produces only radiation down. Figure 3(c) shows the computed complex-wavevector band structure of the grating. Because of the unit cell's asymmetry in coordinate x, the full Brillouin zone of the structure is simulated to obtain all supported modes, including both (1) downward and (2) upward radiating modes. By simulating the complex-wavevector band structure, the radiative properties of the grating unit cell, such as radiation efficiency, angle, and directivity, can be rigorously computed and analyzed at desired real-frequency driving points. The presented results indicate that complex-wavevector band structure is the natural formulation for developing rigorous synthesis algorithms for sophisticated grating designs, such as specifically tapered grating strength and focusing designs, for applications in fiber-to-chip coupling, beam forming, and phased arrays.

Last, we demonstrate, to the best of our knowledge, the first formal computation of a new type of open-system Bloch mode proposed as the basis of recently demonstrated ultra-low-loss waveguide crossing arrays [4,5]. The concept behind this new mode is that a waveguide crossing array is an open system and does not have

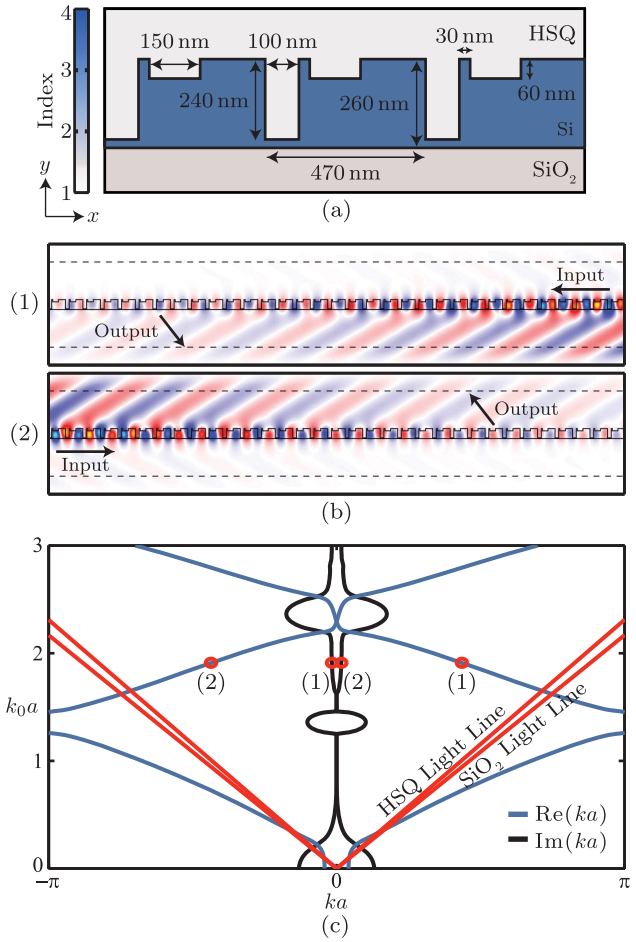

Fig. 3. (a) Three unit cells of a periodic grating coupler [3] showing index distribution and dimensions. (b) Bloch mode profiles of the grating at 1550 nm free-space wavelength for (1) downward and (2) upward radiating modes solved using the proposed FDFD complex-wavevector solver with PML boundaries in y and periodicity in x. (c) Simulated complex-wavevector band structure of the grating with Re(k) in blue and Im(k) in black, HSQ and silica light lines shown, and points analyzed in (b) marked in red.

a simple light line that separates radiation from guidance. Yet, coupling of two modes via scatterers, through an imaginary anti-crossing due to radiative coupling, enables a low-loss Bloch state within the radiation spectrum. Here, we formally compute, for the first time, this low-loss leaky unidirectional breathing Bloch state. Figure 4 shows the simulated field intensity profile of the Bloch-mode crossing design with dimensions chosen to achieve the low-radiation state [5]. In this example, the computed loss per crossing (i.e., per unit cell) is $L_{\mathrm{dB}} = -10\log_{10}(e^{-2\,\mathrm{Im}(ka)}) \approx 0.06$ dB, closely matching results obtained in the initial proposal via FDTD [5]. This complex-wavevector mode solution establishes that this mode of propagation, after imaginary splitting, is a bona fide leaky eigenstate of the system.

As supported by the presented examples and discussion, we believe that complex-wavevector band structure computation has important applications in photonics design. Our finite-difference approach is general, rigorous, scalable, and easily interfaced with FDTD solvers. Extension of the current two-dimensional TE

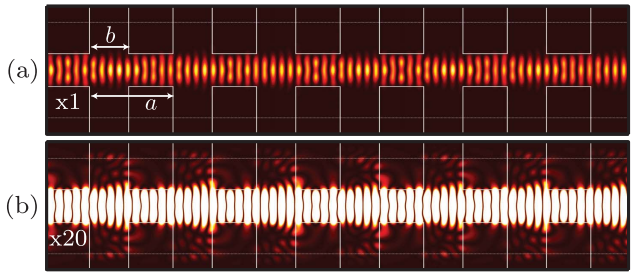

Fig. 4. Low-loss Bloch mode profile intensity, Re(Ψ)^2, of a silicon waveguide crossing array in silica at 1200 nm wavelength simulated with PMLs in y, periodicity in x, $a = 2450$ nm, and $b = 1150$ nm displayed (a) to highlight breathing property and (b) with scaled ordinate range to show minimal loss.

implementation to TM fields and three dimensions is straightforward. We anticipate important applications of this method by building synthesis techniques on top of such band structure solvers that will enable rigorous synthesis of advanced periodic and quasi-periodic photonic devices, including grating couplers, waveguide crossing arrays, and photonic crystals, as well as phased array antennas and other photonic devices.

This work was supported by the National Science Foundation award ECCS-1128709.

References

1. Q. Quan and M. Lončar, Opt. Express **19**, 18529 (2011).
2. D. Taillaert, P. Bienstman, and R. Baets, Opt. Lett. **29**, 2749 (2004).
3. M. Fan, M. A. Popović, and F. X. Kärtner, *Conference on Lasers and Electro-Optics*, OSA Technical Digest (Optical Society of America, 2007), paper CTuDD3.
4. Y. Liu, J. M. Shainline, X. Zeng, and M. A. Popović, Opt. Lett. **39**, 335 (2014).
5. M. A. Popović, E. P. Ippen, and F. X. Kärtner, in *Proceedings of the Annual Meeting of the IEEE Lasers and Electro-Optics Society* (IEEE, 2007), p. 56.
6. J. Orcutt, B. Moss, C. Sun, J. Leu, M. Georgas, J. Shainline, E. Zgraggen, H. Li, J. Sun, M. Weaver, S. Urošević, M. Popović, R. Ram, and V. Stojanović, Opt. Express **20**, 12222 (2012).
7. J. Sun, E. Timurdogan, A. Yaacobi, E. S. Hosseini, and M. R. Watts, Nature **493**, 195 (2013).
8. S. Johnson and J. Joannopoulos, Opt. Express **8**, 173 (2001).
9. A. Archambault, T. V. Teperik, F. Marquier, and J. J. Greffet, Phys. Rev. B **79**, 195414 (2009).
10. A. Parzygnat, K. K. Y. Lee, Y. Avniel, and S. G. Johnson, Phys. Rev. B **81**, 155324 (2010).
11. K. Huang, E. Lidorikis, X. Jiang, J. Joannopoulos, K. Nelson, P. Bienstman, and S. Fan, Phys. Rev. B **69**, 195111 (2004).
12. Y. Ding and R. Magnusson, Opt. Express **15**, 680 (2007).
13. C. Engström, C. Hafner, and K. Schmidt, J. Comput. Theor. Nanosci. **6**, 775 (2009).
14. C. Fietz, Y. Urzhumov, and G. Shvets, Opt. Express **19**, 19027 (2011).
15. G. Parisi, P. Zilio, and F. Romanato, Opt. Express **20**, 16690 (2012).
16. W. Chew, J. Appl. Phys. **75**, 4843 (1994).
17. K. Yee, IEEE Trans. Antennas Propag. **14**, 302 (1966).
18. K. Radhakrishnan and W. C. Chew, IEEE Trans. Microw. Theory Tech. **49**, 1345 (2001).
19. F. Teixeira and W. Chew, IEEE Trans. Antennas Propag. **46**, 1386 (1998).
20. A. Yariv and P. Yeh, *Photonics* (Oxford University, 2007).